 Universidad del Atlántico	CÓDIGO: FOR-DO-109
	VERSIÓN: 0
	FECHA: 03/06/2020
AUTORIZACIÓN DE LOS AUTORES PARA LA CONSULTA, LA REPRODUCCIÓN PARCIAL O TOTAL, Y PUBLICACIÓN ELECTRÓNICA DEL TEXTO COMPLETO	

Puerto Colombia, 4 de abril de 2022

Señores

DEPARTAMENTO DE BIBLIOTECAS

Universidad del Atlántico

Cuidad

Asunto: Autorización Trabajo de Grado

Cordial saludo,

Yo, **LUDIS MERCEDES COBA JIMENEZ**, identificada con **C.C. No. 1.001.994.909** de **BARRANQUILLA**, autora del trabajo de grado titulado **INTERACTION OF CIPROFLOXACIN WITH ARABINOSE, GLUCOSAMINE, GLUCURONIC ACID AND RHAMNOSE: INSIGHTS FROM GENETICALGORITHM AND QUANTUM CHEMISTRY** presentado y aprobado en el año **2022** como requisito para optar al título Profesional de **QUÍMICO**; autorizo al Departamento de Bibliotecas de la Universidad del Atlántico para que, con fines académicos, la producción académica, literaria, intelectual de la Universidad del Atlántico sea divulgada a nivel nacional e internacional a través de la visibilidad de su contenido de la siguiente manera:

- Los usuarios del Departamento de Bibliotecas de la Universidad del Atlántico pueden consultar el contenido de este trabajo de grado en la página Web institucional, en el Repositorio Digital y en las redes de información del país y del exterior, con las cuales tenga convenio la Universidad del Atlántico.
- Permitir consulta, reproducción y citación a los usuarios interesados en el contenido de este trabajo, para todos los usos que tengan finalidad académica, ya sea en formato CD-ROM o digital desde Internet, Intranet, etc., y en general para cualquier formato conocido o por conocer.

Esto de conformidad con lo establecido en el artículo 30 de la Ley 23 de 1982 y el artículo 11 de la Decisión Andina 351 de 1993, “Los derechos morales sobre el trabajo son propiedad de los autores”, los cuales son irrenunciables, imprescriptibles, inembargables e inalienables.

Atentamente,

Firma 

LUDIS MERCEDES COBA JIMENEZ

C.C. No. 1.001.994.909 de BARRANQUILLA

DECLARACIÓN DE AUSENCIA DE PLAGIO EN TRABAJO ACADÉMICO PARA GRADO


Este documento debe ser diligenciado de manera clara y completa, sin tachaduras o enmendaduras y las firmas consignadas deben corresponder al (los) autor (es) identificado en el mismo.

Puerto Colombia, **4 de abril de 2022**

Una vez obtenido el visto bueno del director del trabajo y los evaluadores, presento al **Departamento de Bibliotecas** el resultado académico de mi formación profesional o posgradual. Asimismo, declaro y entiendo lo siguiente:

- El trabajo académico es original y se realizó sin violar o usurpar derechos de autor de terceros, en consecuencia, la obra es de mi exclusiva autoría y detento la titularidad sobre la misma.
- Asumo total responsabilidad por el contenido del trabajo académico.
- Eximo a la Universidad del Atlántico, quien actúa como un tercero de buena fe, contra cualquier daño o perjuicio originado en la reclamación de los derechos de este documento, por parte de terceros.
- Las fuentes citadas han sido debidamente referenciadas en el mismo.
- El (los) autor (es) declara (n) que conoce (n) lo consignado en el trabajo académico debido a que contribuyeron en su elaboración y aprobaron esta versión adjunta.

Título del trabajo académico:	INTERACTION OF CIPROFLOXACIN WITH ARABINOSE, GLUCOSAMINE, GLUCURONIC ACID AND RHAMNOSE: INSIGHTS FROM GENETIC ALGORITHM AND QUANTUM CHEMISTRY
Programa académico:	Química

Firma de Autor 1:							
Nombres y Apellidos:	Ludis Mercedes Coba Jiménez						
Documento de Identificación:	CC	X	CE		PA	Número:	1.001.994.909
Nacionalidad:	Colombiana				Lugar de residencia:	Barranquilla	
Dirección de residencia:	Carrera 18 # 17-56, Villa Norte						
Teléfono:	3003261				Celular:	3013418293	



FORMULARIO DESCRIPTIVO DEL TRABAJO DE GRADO

TÍTULO COMPLETO DEL TRABAJO DE GRADO	INTERACTION OF CIPROFLOXACIN WITH ARABINOSE, GLUCOSAMINE, GLUCURONIC ACID AND RHAMNOSE: INSIGHTS FROM GENETICALGORITHM AND QUANTUM CHEMISTRY
AUTOR(A) (ES)	LUDIS MERCEDES COBA JIMENEZ
DIRECTOR (A)	JULIO ROMÁN MAZA VILLEGAS
JURADOS	ALFREDO PÉREZ GAMBOA ATILANO PASTRANA MARTÍNEZ
TRABAJO DE GRADO PARA OPTAR AL TÍTULO DE	QUÍMICO
PROGRAMA	QUÍMICA
PREGRADO / POSTGRADO	PREGRADO
FACULTAD	CIENCIAS BÁSICAS
SEDE INSTITUCIONAL	SEDE NORTE
AÑO DE PRESENTACIÓN DEL TRABAJO DE GRADO	2022
NÚMERO DE PÁGINAS	7
TIPO DE ILUSTRACIONES	Esquemas, Figuras y Tablas.
MATERIAL ANEXO (VÍDEO, AUDIO, MULTIMEDIA O PRODUCCIÓN ELECTRÓNICA)	NO APLICA
PREMIO O RECONOCIMIENTO	NO APLICA



**INTERACTION OF CIPROFLOXACIN WITH ARABINOSE, GLUCOSAMINE,
GLUCURONIC ACID AND RHAMNOSE: INSIGHTS FROM GENETICALGORITHM AND
QUANTUM CHEMISTRY**

**LUDIS MERCEDES COBA JIMENEZ
TRABAJO DE GRADO PARA OPTAR AL TITULO DE QUÍMICO**

**PROGRAMA DE QUÍMICA
FACULTAD DE CIENCIAS BÁSICAS
UNIVERSIDAD DEL ATLÁNTICO
PUERTO COLOMBIA
2022**



**INTERACTION OF CIPROFLOXACIN WITH ARABINOSE, GLUCOSAMINE,
GLUCURONIC ACID AND RHAMNOSE: INSIGHTS FROM GENETICALGORITHM AND
QUANTUM CHEMISTRY**

**LUDIS MERCEDES COBA JIMENEZ
TRABAJO DE GRADO PARA OPTAR AL TITULO DE QUÍMICO**

**JULIO ROMÁN MAZA VILLEGAS
MAESTRÍA EN CIENCIAS QUÍMICAS – QUÍMICA TEÓRICA**

**PROGRAMA DE QUÍMICA
FACULTAD DE CIENCIAS BÁSICAS
UNIVERSIDAD DEL ATLÁNTICO
PUERTO COLOMBIA
2022**

NOTA DE ACEPTACION

DIRECTOR(A)

JURADO(A)S

■ Electro, Physical & Theoretical Chemistry

Interaction of Ciprofloxacin with Arabinose, Glucosamine, Glucuronic Acid and Rhamnose: Insights from Genetic Algorithm and Quantum Chemistry

Ludis Coba-Jiménez,^[a] Julio Maza,^[a] Mayamarú Guerra,^[b] Julio Deluque-Gómez,^[c] and Néstor Cubillán^{*[a]}

A theoretical study of the ciprofloxacin interactions with glucuronic acid, arabinose, glucosamine, and rhamnose is presented. The most stable complexes were obtained through genetic algorithms starting from the neutral and zwitterion species of ciprofloxacin. The energy at the semiempirical level PM7 of the optimal structures of the complexes was the genetic algorithm's fitness function. The resulting complexes' geometry was optimized at M062X–D3/6-311++G** level of theory, and non-covalent interactions were assessed through the reduced density gradient and quantum theory of atoms in molecules. The results show that the zwitterion species of

ciprofloxacin favorably complex carbohydrates and can induce proton exchange between them. The molecular complexes from proton exchange are the most stable, followed by the complexes formed by the contact of the zwitterion species and the carbohydrate. The complexes formed by both neutral species were the least stable. The medium strength and strong (assisted by charge) hydrogen bonds, the $XH\cdots\pi$ and lone-pair- π interactions, were mainly present in the complexes. Proton exchange processes strengthen the interactions mentioned above.

Introduction

Ciprofloxacin (CIP) is a broad-spectrum antibiotic that has recently aroused interest because of the significant increase in pathogens' antimicrobial resistance, such as *Escherichia coli* and *Neisseria gonorrhoeae*. In Germany and the United Kingdom, the *Escherichia coli* resistance raised to about 15% in 2016 and 30% in Spain.^[1] On the other hand, in Uganda, 60–65% (total population 639) showed *Neisseria gonorrhoeae* evidence from 2016 to 2018, of which 94% was resistant.^[2]

The sales without prescription promote indiscriminate use in agricultural and human activities, increasing the antibiotic presence in water bodies and wastewater treatment plants (WWTPs). After human consumption, the ciprofloxacin excretion is approximately 60% and 20% through urine and feces, respectively.^[3] A recent meta-analysis of CIP concentration studies in the rivers revealed an increment (30.68 to 148.46 ng/

L) between the five-year periods 2007–2011 and 2012–2016.^[4] Moreover, up to 228 ng/L of CIP concentrations were found in WWTP influents; however, the effluents showed 0.9–4.7% in CIP removal.^[5]

There are two ways of tackling this problem, and carbohydrates-based materials have helped. The carbohydrates-based materials are low-cost, efficient, and easy to obtain from natural sources. Besides, carbohydrates are the second biomolecules group adsorbing CIP in sewage sludge^[6] and microalgae.^[7] In both cases, the carbohydrates allow the complexation and further release of CIP.

The first way can be drawn by drug delivery strategies to improve bioavailability. Jung et al. reported an increasing antibacterial activity against methicillin-resistant *Staphylococcus Aureus* by encapsulating CIP with mono-6-deoxy-6-aminoethylamino-cyclodextrin.^[8] Arafa, Mousa, and Afifi found an increasing release of CIP in root canals infected by *E. faecalis* by coating PLGA with chitosan.^[9]

In a second way, carbohydrate-based materials have shown high removal capacity of CIP from water. Chitosan immobilized on MgO nanosheet enhanced the CIP removal capacity of graphene oxide from 50% to approximately 100%.^[10] According to the authors, the immobilization and synergistic effects increase the number of acceptable and available active sites.

The number and heterogeneous nature of functional groups in CIP and carbohydrates suggest how chemical entities associate. The chemical intuition or the analysis of the more significant molecular regions are criteria for designing most interaction models. Thus, the evident electrostatic and weak specific interactions determine the modeling. This approach

[a] L. Coba-Jiménez, Dr. J. Maza, Dr. N. Cubillán
Programa de Química, Facultad de Ciencias Básicas
Universidad del Atlántico
Barranquilla, Colombia
E-mail: nestorcubillan@mail.uniatlantico.edu.co

[b] Dr. M. Guerra
Laboratorio de Óptica y Procesamiento de Imágenes, Facultad de Ciencias Básicas
Universidad Tecnológica de Bolívar
Turbaco, Colombia

[c] J. Deluque-Gómez
Programa de Ingeniería Industrial, Facultad de Ingenierías
Universidad de la Guajira
Riohacha, Colombia

Supporting information for this article is available on the WWW under <https://doi.org/10.1002/slct.202103836>

avoids exploring the possible cooperativity between electrostatics, specific and nonspecific weak interactions.

Genetic Algorithms have been helpful to analyze different interaction modes between molecules by optimizing the interaction energy or related function. Molecular Docking is a straightforward application of Genetic Algorithms; however, improving scoring functions accuracy is mandatory.^[11] A compromise between accuracy and computer time becomes necessary, e.g., semiempirical energies enhance the Molecular Docking accuracy in proteins.^[12]

In the literature, the discussion about the Molecular Docking complexes is performed by comparing atomic distances and the overall interaction energy. The comparison with the experiment usually confirms most theoretical studies of CIP complexes with carbohydrates-based materials.^[8,13]

The modern Quantum Chemistry methodologies for studying non-covalent interactions allow the in-depth analysis of underlying forces addressing the complex formation. The Quantum Theory of Atom in Molecules (QTAIM) and the reduced density gradient (RDG) are methods based on the electron density topology. From QTAIM, the zero-flux surface of electron density divides molecules or complexes into fragments linked by their critical points. The QTAIM molecular graph allows for identifying and quantifying specific (e.g., hydrogen bonds) and some nonspecific (e.g., localized $\pi\cdots\pi$) non-covalent interactions. RDG plots characterize and locate non-covalent interactions invisible to QTAIM in the molecular real-space.^[14]

Based on these facts, a thorough analysis of CIP-carbohydrates interaction's modes and intrinsic forces becomes necessary. This knowledge will contribute to understanding CIP adsorption mechanisms and, consequently, the design of new CIP delivery and removal materials.

In this work, we explored by Genetic Algorithms the interaction modes of CIP and CIP[±] with rhamnose (RH), glucosamine (GA), glucuronic acid (AG), and arabinose (AR) as representative carbohydrates from natural sources. The interaction energy distribution analysis conducted the interpretation of these results. The purpose was to identify the more important CIP-saccharide complexes. Furthermore, the non-covalent interactions were quantified and classified with QTAIM, reduced density-gradient interactions, and multivariate analysis. The contributions of relevant functional groups and the electrostatic nature were the central topics for discussing the origin of the interactions.

Results and Discussion

Evolutionary searching of Interaction Complexes

Genetic algorithms are population-based metaheuristic methods simulating the evolution process. These methods allow exploring a broad region of feasible solutions. In this regard, it is possible to obtain a set of structures in a global or local energy minimum, i.e., the more stable complexes. CIP interacted in the neutral (CIP) and zwitterion (CIP[±]) charge state – labeled as CP and CZ, respectively.

Figure 1 shows the evolution of the most-stable complexes of CIP and CIP[±] with monosaccharides as obtained by Genetic Algorithms. There is no apparent influence of mating probability calculated from Normal (Fps, Equation E1, supplementary information, section SM1.1) and Boltzmann (Bps, Equation E2, supplementary information, section SM1.1) distributions. Similarly, there are no differences in the evolution of CIP and CIP[±] interacting with all carbohydrates.

The convergence is rapidly reached at generations lesser than 20. However, we observed several exceptions, CIP[±]/GA(Bps), CIP[±]/RH(Fps), and CIP[±]/AR (Fps), where the convergence was obtained after 30 generations. AG and GA found the convergence faster than the others (see Figure 1A and 1C). Probably, the electrostatic interaction induced by the carboxylic and amine groups – greater than the OH groups in RH and AR – increased the convergence pressure.

The interaction-energy distributions of the last population for each CIP-carbohydrate pair are observed in Figures S1–S4. In all cases, the results behaved as multimodal distributions were obtained, as observed in the multiple-Gaussians fitting results in Table S1. The determination coefficient was greater than 0.99.

Although the different mating probabilities, the distributions were quite similar. The Boltzmann probability induces high convergence pressure in roulette selection, but diversity can be affected. The clone deletion and the relatively high mutation probability appear to keep the population diversity in this work. Therefore, the relative frequency of the appearance of the more stable complexes decreased. However, the elitism helped us to preserve the better individuals.

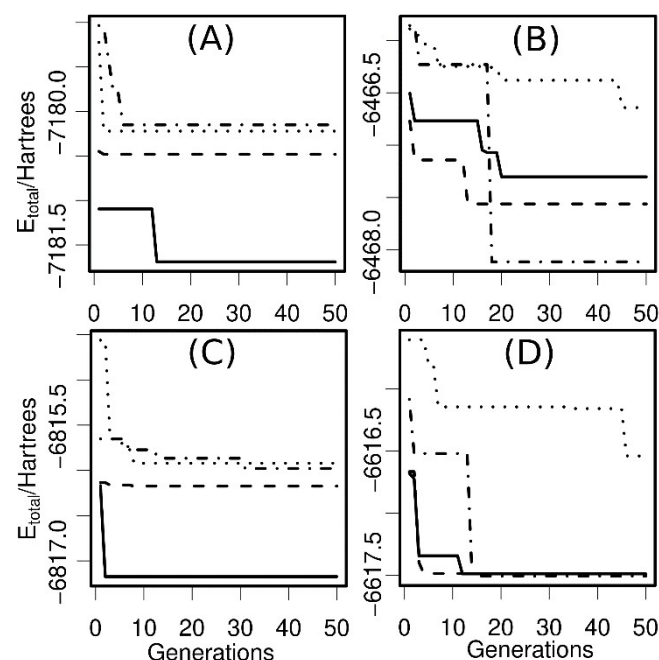


Figure 1. Evolution of CIP and CIP[±] interactions with different carbohydrates. CH: Carbohydrate type. – CIP/CH (Fps); - - - CIP/CH (Bps); ... CIP[±]/CH (Fps); - · - · CIP[±]/CH (Bps). (A) AG: Glucuronic acid, (B) AR: Arabinose, (C) GA: Glucosamine, (D) RH: Rhamnose.

Molecular Models of Interaction Complexes

The more representative interaction modes of CIP with carbohydrates (CH) show the existence of neutral (CIP), zwitterion (CIP[±]), negative (CIP⁻), and positive (CIP⁺) forms of ciprofloxacin in the complexes. Four molecular complex models were identified and labeled CIP/CH, CIP[±]/CH, CIP⁺/CH⁻, and CIP⁻/CH⁺. Figure 2 shows the low-energy complexes of the before-mentioned interaction models obtained by Genetic Algorithms and the analysis of interaction-energy distributions (Supplementary information, section SM2).

The interaction energy (E_{int}) was calculated as represented in Scheme 1. The most-stable CIP and CH geometrically rearrange towards a conformation suitable for the complex formation-in-complex geometry. These reorganization energies, R_{CIP} and R_{CH} , are the energy difference between the optimized (E_{CIP} and E_{CH}) and in-complex (E_{CIP}^* and E_{CH}^*) geometries, respectively.

Furthermore, compounds in complex geometry (CIP* and CH*) form the complex (CIP·CH). The difference between the

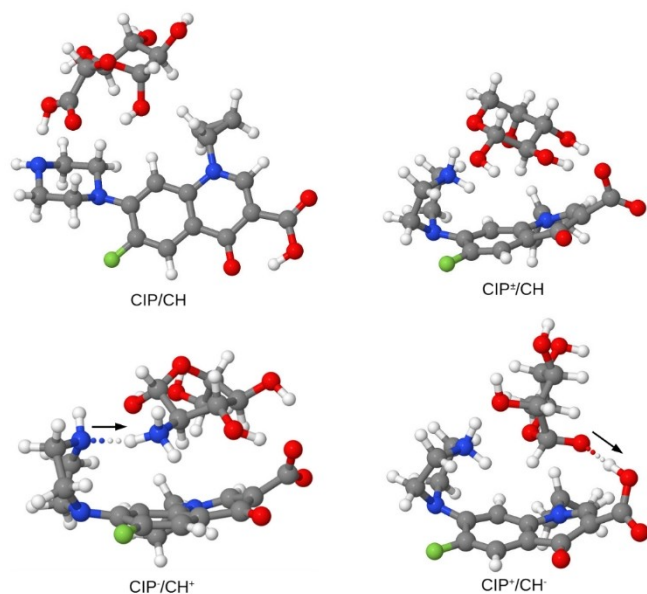
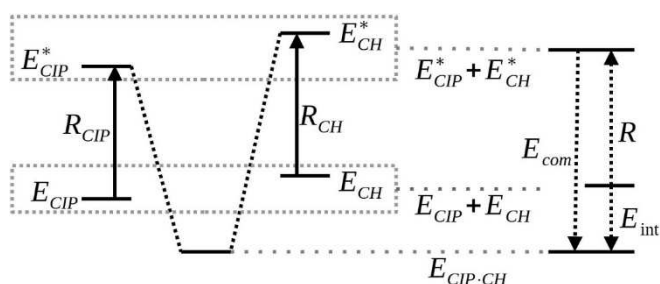


Figure 2. Low-energy molecular complexes representative of the CIP/CH, CIP[±]/CH, CIP⁺/CH⁻, and CIP⁻/CH⁺ interactions. The arrows in CIP⁺/CH⁻ and CIP⁻/CH⁺ signal the proton transfer direction.



Scheme 1. Interaction energy definition.

energies of the isolated CIP and CH in complex conformation (E_{CIP}^* and E_{CH}^*) and the energy of the complex ($E_{CIP·CH}$) defined the complexation energy (E_{com}):

$$E_{com} = E_{CIP·CH} - E_{CIP}^* - E_{CH}^* \quad (1)$$

Finally, the interaction energy (E_{int}) is calculated as follow:

$$E_{int} = E_{CIP·CH} - E_{CIP} - E_{CH} \quad (2)$$

The values of E_{com} , E_{intr} , E_{CIP}^* , E_{CH}^* , E_{CIP} , and E_{CH} of all complexes are shown in Table S2 (Supplementary information, section SM1.1). Figures 3 and 4 summarize the results presented in this table. The interaction energy distributions showed skewness; in this sense, all comparisons were realized by median instead of mean.

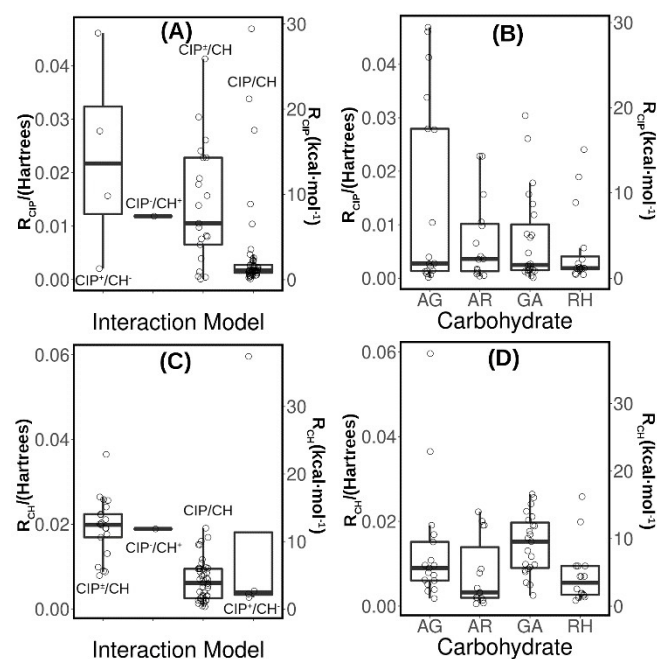


Figure 3. Conformational reorganization energies of CIP and Carbohydrates as function of interaction type and carbohydrate nature.

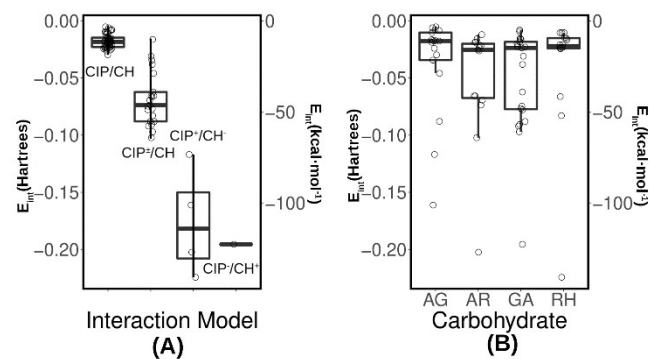


Figure 4. The interaction energy of complexes between CIP and carbohydrates as function of the interaction model and carbohydrate nature.

The total contribution of the reorganization energy on E_{int} was relatively low, as expected.^[15] The median and mean of E_{int} and E_{com} differ by 7.4 and 12.6 kcal/mol, respectively.

The R_{CIP} and R_{CH} depend on the electrostatic behavior in the complexation. The ion-exchange processes (CIP^+/CH^- and CIP^-/CH^+) given higher R_{CIP} median values, 13.6 and 7.4 kcal/mol, respectively. Furthermore, the Zwitterion interaction (CIP^\pm/CH) induced median CIP reorganization energies of 6.6 kcal/mol. The lower R_{CIP} were obtained for the neutral interaction, CIP/CH (1.1 kcal/mol). – see Figure 3A. Conversely, R_{CIP} showed no influence of the carbohydrate nature, between 1.1–2.2 kcal/mol (Figure 3B).

R_{CH} showed no dependence on the electrostatic behavior (Figure 3C). The CIP^+/CH^- and CIP/CH interaction promoted lower carbohydrate reorganization (<4.2 kcal/mol) while the rest of the interaction types reached between 11.0 and 12.1 kcal/mol. Apart, the nature of the carbohydrate also influenced its reorganization energy reinforcing the idea of the contribution of electrostatic forces. AG and GA are more reorganized (5.6 and 9.5 kcal/mol) than RH and AR (3.5 and 2.0 kcal/mol) (see Figures 3C and 3D).

In our case, it is possible to suggest that electrostatic interactions drive these conformational changes in the interaction process. Noresson et al. found similar results, enhancing the affinity of ligand-protein interactions.^[16] In another report, the insertion of a sulfate group in a mono-galactoside model promoted the side-chain guanidine movement to obtain close-range electrostatic interactions. In natural systems, the interactions follow the principle of minimal frustration where the process path minimizes the conformational barriers.^[17]

The values of E_{int} ranged between –3.3 and –140.7 kcal/mol. The neutral CIP/CH interaction showed the higher interaction energies (–3.3––18.7 kcal/mol, median –11.6 kcal/mol, Figure 4A). These values are in the same E_{int} magnitude order as the CIP interactions with graphene oxide and boron nitride oxide nanoflakes (–4.84271 and –9.45482 kcal/mol, respectively) at PBE/DZP level of theory.^[18] The Zwitterion interaction (CIP^\pm/CH) decreased E_{int} (–46.2 kcal/mol, Figure 4A). Similar behavior has been observed with molecular dynamics for the interaction of CIP with carbon nanotubes where E_{int} changed from –24.9 (CIP) to –26.8 (CIP^\pm) kcal/mol.^[19]

Furthermore, the lower E_{int} values were found for complex involving charged species, CIP^+/CH^- (–110.5 kcal/mol) and CIP^-/CH^+ (–122.6 kcal/mol). In fact, our calculations suggest that CIP can transfer a proton to GA, and CIP^\pm to accept a proton from AR, GA, and RH (see Figure 2). In these proton transfers, E_{int} fell between –110 and –120 kcal/mol. According to Cheng et al., the CIP adsorption in swine manure undergoes cation-exchange complexation-reaction rather than electrostatic interactions.^[20] Moreover, Zhao et al. suggested that CIP accepts H^+ from media water before interacting with graphene by cation- π interactions.^[21]

The median of $E_{int}E_{int}$ showed subtle differences varying the carbohydrate (Figure 4B): AR (–16.0 kcal/mol) < GA (–14.9 kcal/mol) < RH (–13.9 kcal/mol) < AG (–11.2 kcal/mol). However, the differences between lower E_{int} values were marked: RH (–0.22 kcal/mol) < AR (–0.20 kcal/mol) \approx GA (–0.20 kcal/mol) < AG (–0.16 kcal/mol), see Figure 4B. In all cases, the interaction involved ion-exchange.

Non-covalent interactions

Electron density topology consistency were ensured by the Poincaré-Hopf rule's completeness for all QTAIM molecular graphs from the modelled complexes. Table 1 shows the QTAIM properties critical points (CP) of molecular complexes conforming groups obtained by Hierarchical Clustering methods. Groups 1 and 2 have similar QTAIM properties (see dendrogram from the hierarchical cluster analysis, supplementary information, Figure S36). These groups included critical points with low densities (0.00008–0.02 au). In both groups, closed-shell interactions are involved ($|V|/G < 1$).^[22] The ellipticity values are associated with symmetric and asymmetric charge distribution range ($0.015 \leq \varepsilon \leq 4.208$). Group 6 differ from 1 and 2 by critical points with high density-asymmetry, $\varepsilon > 2.68$, indicating bonding interaction instability due to the low density values within the limit of the numerical differentiation procedures of MultiWFN.^[23,24]

The Electron Localization Function (ELF) and Localized Orbital Locator (LOL) values reproduce the closed-shell nature of the bonding interactions pointed out by the QTAIM analysis. Moreover, the ELF values correlate with symmetric electron

Table 1. Density(ρ , au), Density laplaciano($\nabla^2\rho$, au), Potential energy density(V , au), Lagrangian kinetic energy(G , au), Espinosa's relation,^[34] $|V|/G$, Energy density(H_c , au), Ellipticity(ε), Electron localization function(ELF), Localized orbital locator(LOL), Local information entropy(LIE) and Average locale ionization energy(ALIE) of the critical points (CP) of molecular complexes conforming groups obtained by Hierarchical Clustering methods Table Caption.

Group	1	2	3	4	5	6
$\rho \cdot 10^2$	0.20–1.94	0.08–1.20	5.86–9.39	2.11–3.46	3.30–5.39	0.19–1.17
$\nabla^2\rho \cdot 10^2$	0.80–7.75	0.33–4.25	7.72–15.17	7.43–13.79	8.85–15.64	0.64–4.39
$-V \cdot 10^2$	1.42–0.11	0.80–0.03	10.97–5.24	3.07–1.59	5.63–2.53	0.82–0.09
$G \cdot 10^2$	0.16–1.66	0.06–0.93	3.63–6.97	1.72–3.16	2.22–4.77	0.12–0.96
$ V /G$	0.73–0.94	0.51–0.92	1.27–1.57	0.868–0.999	1.02–1.31	0.72–0.90
$H_c \cdot 10^3$	0.35–2.75	0.24–1.32	(–40.0)–(–13.1)	0.014–2.72	(–10.5)–(–0.5)	0.35–1.74
ε	0.015–4.208	0.021–3.017	0.008–0.073	0.019–0.207	0.006–0.083	2.678–16.358
ELF	0.0035–0.0694	0.0012–0.0543	0.2214–0.3891	0.0585–0.1176	0.1184–0.2576	0.0046–0.0398
LOL	0.056–0.215	0.034–0.194	0.348–0.444	0.200–0.268	0.268–0.371	0.064–0.169
LIE $\cdot 10^5$	0.89–7.04	0.37–4.62	18.13–28.43	7.31–11.49	10.85–17.80	0.84–4.47
ALIE	0.48–0.72	0.43–0.56	0.55–0.68	0.52–0.70	0.53–0.70	0.44–0.61

density charge distribution,^[25] whereas ELF index unveils electronic charge localization (i.e., higher ELF values) as the numerical values for ellipticity goes close to zero (Groups 3–5).

The number of CPs found in the clustered complexes implies intermolecular interactions and their characteristics, open or closed-shell interactions. Groups 1 and 2 show the highest number of bonding interactions present (see supplementary information Figure S36), compared to Groups 3 to 6. Table 1 unveils the closed-shell interactions nature in clusters Group 1, 2, and 6. However, the interactions' instability in Group 6 is the key to ruling out the constructive interactions that add to the complex formation, leaving the characterized interactions for Groups 1 and 2 as the more stabilizing interactions. The extend of the closed-shell interactions for the molecular complexes goes beyond explaining the contribution to molecular stability in isolation (a closed-shell interaction with $\rho \approx 0.6$ a.u. roughly contributes with a bond energy of ~ 1 kcal/mol).^[26] Thus, the different interaction models will potentiate the progressive effect of the intermolecular interactions modeled by the theoretical approach.

Figure 5 shows NCIPLOTs and QTAIM molecular graphs of the low-energy complexes representing CIP/CH, CIP $^{\pm}$ /CH, CIP $^{+}$ /CH $^{-}$, and CIP $^{-}$ /CH $^{+}$ interactions. The RDG isosurfaces and RDG vs. $\text{sign}(\lambda_2)\rho$ plot (NCIPLOTs) identify these regions as van der Waals type interactions. All obtained molecular complexes results are in Supplementary information, Figures S20–S35 and Table S2.

The H $\cdots\pi$ and lone-pair $\cdots\pi$ interactions are observed as “funnel-like” RDG isosurfaces.^[27] These fragments resemble the traditional T-shaped and tilted T-shaped edge-to-face orientation of anion/cation/lone-pair $\cdots\pi$ interaction.^[28] From these interactions, the T-shaped is the most stable.^[29] The $\text{sign}(\lambda_2)\rho$ values characterized these as dispersion interactions (< 0.01 au).^[30]

The complexes CZGA_f03 and CZRH_f03 clearly show these interactions, and to a lesser extent, CZAR_b01 (Figure 5). It is noteworthy the ion exchange influence the relative strength of these interactions. In CZGA_f03, the two CH $\cdots\pi$ interactions – associated with the CP's B03 and B04 – had ρ of 0.008 and 0.009 au, respectively, and ellipticities around 1.0. In CZRH_f03, the ρ fell to 0.006, and the ellipticity increased to 2.0. On the other hand, in CZAR_b01, the ρ was similar to CZRH_f03, but the π contribution decreased to $\varepsilon = 0.55$ (CP B03).

Kozmon et al.^[31] and Jiménez-Moreno et al.^[32] found a direct dependence of CH $\cdots\pi$ density with interaction energy. In our case, the results suggest that coulomb interactions and ion-exchange processes induced the CH $\cdots\pi$ interactions. It is possible because the π hole on the CIP aromatic moiety interacts with lone-pairs^[33] and CH^[32] as a consequence of the fragment proximity. CZRH_f03 is more stable than CZGA_f03 by ca. 18 kcal/mol (see Table S2), but the former contains one CH $\cdots\pi$ contact while the last 2 CH $\cdots\pi$ contacts.

Consequently, the lone-pair $\cdots\pi$ interactions are also possible in these complexes. Hydroxyl oxygen atoms from carbohydrates are involved in these contacts, e.g., CZGA_f03, CZAG_

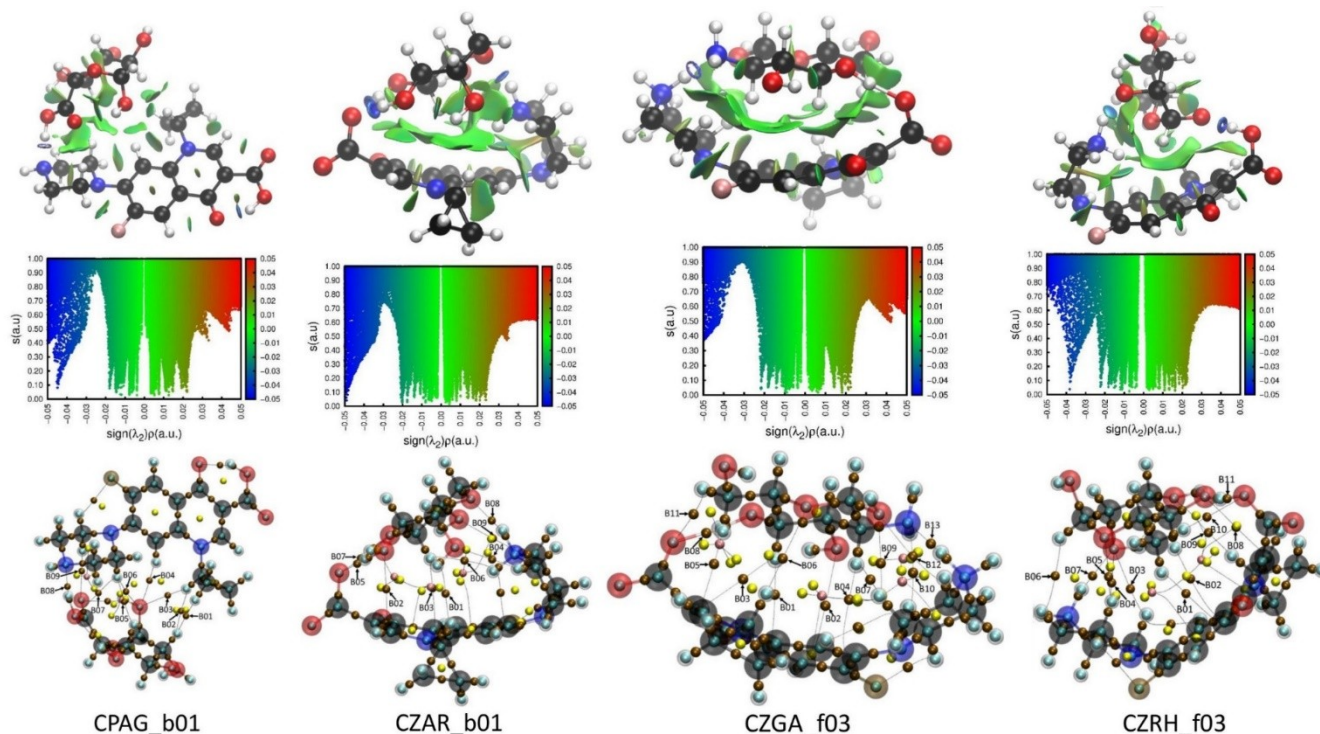


Figure 5. RDG isosurfaces, RDG vs. $\text{sign}(\lambda_2)\rho$ plots and QTAIM molecular graphs for the low-energy complexes representing CIP/CH, CIP $^{\pm}$ /CH, CIP $^{+}$ /CH $^{-}$, and CIP $^{-}$ /CH $^{+}$ interactions. Small spheres in QTAIM molecular graphs represent the critical points: cyan, ochre, yellow and pink spheres locate the nuclear (3,–3), bond (3,–1), ring (3,+1) and cage (3,+3) critical points, respectively.

b04, and CZAR_b03 (see Figures.S20–S35). On the other hand, ether oxygen barely participates in lone-pair... π interaction; only two cases were observed CPAG_b05 and CPAG_f03.

Other H... π interactions that are scarcely present in the complexes are NH... π (CZGA_b01) and OH... π (CPAR_{f02,f03}). Probably, the electrostatic potential on the aromatic centers not favored the π donation towards hydrogen as commonly occur.^[35]

The hydrogens bonds appear below -0.02 au of $\text{sign}(\lambda_2)\rho$. The relative strength of these interactions has been associated with the $\text{sign}(\lambda_2)\rho$, thus, the color in the colormap.^[36] The Hierarchical Clustering Analysis classified these hydrogen bonds in three groups 3–5, see Table 1. These groups are identified by three regions in ρ , 0.021 – 0.034 (4), 0.033 – 0.054 (5), 0.059 – 0.094 (3) au.

The first cluster is associated with moderate hydrogen bonds containing closed-shell interactions ($|V|/G < 1$, $H_c > 0$). The second (5) and third (3) clusters represent partially covalent hydrogen bonds ($1 \leq |V|/G \leq 2$, $H_c < 0$, $0.030 \leq \rho \leq 0.039$).

According to Rozas et al., classification corresponds to medium strength (group 4, Table 1) and strong hydrogen bonds (group 3 and 5, Table 1), respectively.^[34,37] The difference between groups 3 and 5 is attributed to the electron localization degree in the interaction (ELF, LOL, and H_c).

RDG vs. $\text{sign}(\lambda_2)\rho$ and NCIPLOT did not show the stronger interactions (group 3, $\rho > 0.075$ au, Table 1), supporting the effect of the observed covalency contribution in these interactions. Two examples can be observed in Figure 5, OH...O in CZAG_f03 (CP B08) and OH...O in CZRH_f03 (CP B11). These interactions are related to ion-exchange processes; consequently, it is possible to classify them as charge-assisted hydrogen bonds.^[38]

The functional groups actively participating in hydrogen bonds are carboxyl(ate) and amine (or ammonium) in CIP, while the OH groups are the main interaction regions of carbohydrates. Carboxyl(ate) and amine (or ammonium) in AG and GA also participate in the hydrogen bonds formation. These results support the findings by Xie et al.^[7] where the amine and -OH FTIR/RAMAN bands of *Chlamydomonas* sp. decreased in the presence of CIP. The authors proposed that the adsorption process is addressed by the electrostatic neutralization between the negatively charged surface and positively charged CIP.

Furthermore, Cramariuc et al. by molecular dynamics simulations found CIP favorably interacted with the lipid head groups by hydrogen bonds (phosphate – piperazine nitrogen). The CIP entered to lipid bilayer through hydrogens bonds between CIP carboxylic and lipid esters groups. Conversely, CIP $^{\pm}$ remained in water as stacked aggregates.^[39]

A priori knowledge of types, modes, and relative strength of interactions between CIP and carbohydrates is useful in comprehending removal processes by adsorption mechanisms in biomass. Moreover, the design of synthetic adsorbent can be addressed by the interactions nature depending on the application.

Conclusion

A theoretical study was carried out of the ciprofloxacin interactions with glucuronic acid, arabinose, glucosamine, and rhamnose. The most energetically stable complexes were obtained through genetic algorithms starting from ciprofloxacin's neutral and zwitterionic charge states. The results revealed an important contribution of electrostatic forces in complex formation. The ciprofloxacin zwitterion species favorably form complexes and can induce proton exchange between ciprofloxacin and the carbohydrate. The molecular complexes from proton exchange are the most energetically stable, followed by the complexes formed by the contact of the zwitterion species and the carbohydrate. The complexes formed by both neutral species were the least energetically stable. The medium strength and strong (assisted by charge) hydrogen bonds, XH... π and lone-pair... π the interactions were mainly present in the complexes. Proton exchange processes strengthen the interactions mentioned above.

Supporting Information Summary

The section SM1 summarizes the computational details of Genetic Algorithms (section SM1.1) and DFT calculations (section SM1.2 and SM1.3). The Figures S5–S19 in the section SM2.2 shows the final complexes obtained after interaction energy distributions analysis. In this section, the Table S2 contains the interaction energies of the mentioned complexes. The RDG and QTAIM plots have been located in Figures S20–S35 (section SM3.1). Finally, the section SM3.2 shows the hierarchical clustering for QTAIM results. Additionally, an excel file contains several QTAIM properties of the critical points in the complexes.

Acknowledgements

This research was financially supported by the Ministerio de Ciencias, Tecnología e Innovación de Colombia, Project No. 64514: "Remoción de antibióticos mediante la biomasa residual de microalgas después de extracción de lípidos". N. Cubillán thanks Dr. Muammar El-Khatib (Bristol-Myers-Squibb) and Dr. Alfonso Ballestas-Barrientos by helpful comments and suggestions, and Dr. Jhon Zapata (Universidad de los Andes) by its valuable collaboration with its computational facilities.

Conflict of Interest

The authors declare no conflict of interest.

Data Availability Statement

The data that support the findings of this study are available in the supplementary material of this article.

Keywords: Ciprofloxacin · Carbohydrates · Genetic algorithms · Noncovalent interactions · QTAIM

- [1] A. E. Stapleton, F. M. E. Wagenlehner, A. Mulgirigama, M. Twynholm, *Antimicrob. Agents Chemother.* **2020**, *64*, 1–11.
- [2] M. Unemo, D. Golparian, D. W. Eyre, Humana, in *Neisseria Gonorrhoeae*, Vol. 1 (Ed.: M. Christodoulides), Springer, New York, **2019**, 37–58.
- [3] T. Bergan, A. Dalhoff, R. Rohwedder, *Infect.* **1988**, *16*, S3–S13.
- [4] M. Sarafraz, S. Ali, M. Sadani, Z. Heidarinejad, A. Bay, Y. Fakhri, A. Mousavi Khaneghah, *Int. J. Environ. Anal. Chem.* **2020**, doi:10.1080/03067319.2020.1791330.
- [5] A. S. Ajibola, O. A. Amoniyani, F. O. Ekoja, F. O. Ajibola, *Arch. Environ. Contam. Toxicol.* **2021**, *80*, 389–401.
- [6] K. Wang, D. Gao, J. Xu, L. Cai, J. Cheng, Z. Yu, Z. Hu, J. Yu, *Environ. Sci. Pollut. Res.* **2018**, *25*, 35064–35073.
- [7] P. Xie, C. Chen, C. Zhang, G. Su, N. Ren, S. H. Ho, *Water Res.* **2020**, *172*, 115475.
- [8] J. hyuk Yu, B. Lee, D. Jeong, S. Jung, *Carbohydr. Polym.* **2017**, *163*, 118–128.
- [9] M. G. Arafa, H. A. Mousa, N. N. Afifi, *Drug Delivery* **2019**, *27*, 26–39.
- [10] M. Nazraz, Y. Yamini, H. Asiabi, *Microchim. Acta* **2019**, *186*, 1–9.
- [11] T. Li, R. Guo, Q. Zong, G. Ling, *Carbohydr. Polym.* **2022**, *276*, 118644.
- [12] Z. Bikadi, E. Hazai, *J. Cheminformatics* **2009**, *1*, 1–16.
- [13] Z. Aytac, S. Ipek, I. Erol, E. Durgun, T. Uyar, *Colloids Surf. B* **2019**, *178*, 129–136.
- [14] R. Laplaza, F. Peccati, R. A. Boto, C. Quan, A. Carbone, J.-P. Piquemal, Y. Maday, J. Contreras-García, *Wiley Interdiscip. Rev.: Comput. Mol. Sci.* **2021**, *11*, e1497.
- [15] A. Y. Timoshkin, E. I. Davydova, T. N. Sevastianova, A. V. Suvorov, H. F. Schaefer, in *Int. J. Quantum Chem.*, John Wiley & Sons, Ltd, **2002**, 436–440.
- [16] A. L. Noresson, O. Aurelius, C. T. Öberg, O. Engström, A. P. Sundin, M. Håkansson, O. Stenström, M. Akke, D. T. Logan, H. Leffler, U. J. Nilsson, *Chem. Sci.* **2018**, *9*, 1014–1021.
- [17] J. N. Onuchic, P. G. Wolynes, *Curr. Opin. Struct. Biol.* **2004**, *14*, 70–75.
- [18] E. Duverger, F. Picaud, *J. Mol. Model.* **2020**, *26*, 1–10.
- [19] D. Veclani, A. Melchior, *J. Mol. Liq.* **2020**, *298*, 111977.
- [20] D. Cheng, Y. Feng, Y. Liu, J. Li, J. Xue, Z. Li, *Sci. Total Environ.* **2018**, *634*, 1148–1156.
- [21] Q. Zhao, S. Zhang, X. Zhang, L. Lei, W. Ma, C. Ma, L. Song, J. Chen, B. Pan, B. Xing, *Environ. Sci. Technol.* **2017**, *51*, 13659–13667.
- [22] E. Espinosa, I. Alkorta, J. Elguero, E. Molins, *J. Chem. Phys.* **2002**, *117*, 5529.
- [23] S. Jenkins, J. R. Maza, T. Xu, D. Jiajun, S. R. Kirk, *Int. J. Quantum Chem.* **2015**, *115*, 1678–1690.
- [24] J. Klein, H. Khartabil, J. C. Boisson, J. Contreras-García, J. P. Piquemal, E. Hénon, *J. Phys. Chem. A* **2020**, *124*, 1850–1860.
- [25] B. Silvi, H. Ratajczak, *Phys. Chem. Chem. Phys.* **2016**, *18*, 27442–27449.
- [26] C. F. Matta, N. Castillo, R. J. Boyd, *J. Phys. Chem. B* **2005**, *110*, 563–578.
- [27] D. Dey, D. Chopra, *CrystEngComm* **2017**, *19*, 47–63.
- [28] M. Morales-Toyo, S. Kansız, N. Dege, C. Glidewell, A. Fuenmayor-Zafra, N. Cubillán, *Chem. Phys.* **2021**, *544*, 111119.
- [29] M. Alonso, T. Woller, F. J. Martín-Martínez, J. Contreras-García, P. Geerlings, F. De Proft, *Chem. A Eur. J.* **2014**, *20*, 4931–4941.
- [30] M. D. Esrafil, S. Qasemsolb, *Struct. Chem.* **2017**, *28*, 1255–1264.
- [31] S. Kozmon, R. Matuška, V. Spiwok, J. Koča, *Phys. Chem. Chem. Phys.* **2011**, *13*, 14215–14222.
- [32] E. Jiménez-Moreno, G. Jiménez-Osés, A. M. Gómez, A. G. Santana, F. Corzana, A. Bastida, J. Jiménez-Barbero, J. L. Asensio, *Chem. Sci.* **2015**, *6*, 6076–6085.
- [33] J. Novotný, S. Bazzi, R. Marek, J. Kozelka, *Phys. Chem. Chem. Phys.* **2016**, *18*, 19472–19481.
- [34] S. J. Grabowski, *Chem. Rev.* **2011**, *111*, 2597–2625.
- [35] A. F. Rodrigues-Oliveira, P. R. Batista, L. C. Ducati, T. C. Correra, *Theor. Chem. Acc.* **2020**, *139*, 130.
- [36] J. Contreras-García, W. Yang, E. R. Johnson, *J. Phys. Chem. A* **2011**, *115*, 12983–12990.
- [37] I. Rozas, I. Alkorta, J. Elguero, *J. Am. Chem. Soc.* **2000**, *122*, 11154–11161.
- [38] A. H. Pakiari, K. Eskandari, *J. Mol. Struct.* **2006**, *759*, 51–60.
- [39] O. Cramariuc, T. Rog, M. Javanainen, L. Monticelli, A. V. Polishchuk, I. Vattulainen, *Biochim. Biophys. Acta Biomembr.* **2012**, *1818*, 2563–2571.

Submitted: October 28, 2021

Accepted: December 24, 2021